

Deformation of a single mouse oocyte in a constricted microfluidic channel

ZhengYuan Luo^{1,2} · Sinan Güven^{1,4,6} · Irep Gozen¹ · Pu Chen^{1,4} · Savas Tasoglu^{1,5} · Raymond M. Anchan³ · BoFeng Bai² · Utkan Demirci^{1,4}

Received: 20 November 2014 / Accepted: 21 June 2015 / Published online: 29 July 2015
© Springer-Verlag Berlin Heidelberg 2015

Abstract Single oocyte manipulation in microfluidic channels via precisely controlled flow is critical in microfluidics-based in vitro fertilization. Such systems can potentially minimize the number of transfer steps among containers for rinsing as often performed during conventional in vitro fertilization and can standardize protocols by minimizing manual handling steps. To study shape deformation of oocytes under shear flow and its subsequent impact on their spindle structure is essential for designing microfluidics for in vitro fertilization. Here, we developed a simple yet powerful approach

to (1) trap a single oocyte and induce its deformation through a constricted microfluidic channel, (2) quantify oocyte deformation in real time using a conventional microscope and (3) retrieve the oocyte from the microfluidic device to evaluate changes in their spindle structures. We found that oocytes can be significantly deformed under high flow rates, e.g., 10 $\mu\text{L}/\text{min}$ in a constricted channel with a width and height of 50 and 150 μm , respectively. Oocyte spindles can be severely damaged, as shown here by immunocytochemistry staining of the microtubules and chromosomes. The present approach can be useful to investigate underlying mechanisms of oocyte deformation exposed to well-controlled shear stresses in microfluidic channels, which enables a broad range of applications for reproductive medicine.

Electronic supplementary material The online version of this article (doi:10.1007/s10404-015-1614-0) contains supplementary material, which is available to authorized users.

✉ Utkan Demirci
utkan@stanford.edu

¹ Division of Biomedical Engineering, Department of Medicine, Brigham and Women's Hospital, Harvard Medical School, Boston, MA 02139, USA

² State Key Laboratory of Multiphase Flow in Power Engineering, Xi'an Jiaotong University, Xi'an 710049, People's Republic of China

³ Center for Infertility and Reproductive Surgery, Obstetrics Gynecology and Reproductive Biology, Brigham and Women's Hospital, Harvard Medical School, Boston, MA, USA

⁴ Demirci Bio-Acoustic MEMS in Medicine (BAMM) Lab, Department of Radiology, Canary Center for Early Cancer Detection, Stanford University School of Medicine, Stanford, CA 94304, USA

⁵ Present Address: Department of Mechanical Engineering, University of Connecticut, 191 Auditorium Road, Unit 3139, Storrs, CT 06269-3139, USA

⁶ Present Address: Izmir Biomedicine and Genome Center, Dokuz Eylul University, 35340 Izmir, Turkey

Keywords Oocyte deformation · Spindle damage · Single cell trapping · Microfluidics

1 Introduction

Single cell manipulation enables studying the behavior of individual cells and is widely used for in vitro applications (El-Ali et al. 2006; Vanapalli et al. 2009; Tasoglu et al. 2013a), such as oocyte handlings and transfers that are challenging and operator dependent. Single cell manipulation plays an important role in assisted reproductive technologies (ART). Intracytoplasmic sperm injection (ICSI) is a widely used ART, during which single oocytes are manipulated in vitro, impregnated using intracytoplasmic injection of carefully selected motile sperm (Tasoglu et al. 2013b; Asghar et al. 2014) and cultured until the production of preimplantation-stage embryos. Of note, there is significant requisite manipulation of oocytes during the various steps of in vitro fertilization including oocyte

retrieval, fertilization and embryo culturing. Such extensive micromanipulation of oocytes may induce epigenetic changes as well as injury to cytoskeletal architecture and even oocyte degeneration (Lathi and Milki 2004).

Microfluidic technologies significantly improve fluid control and medium exchange (Gurkan et al. 2012; Rizvi et al. 2013) and therefore would potentially eliminate the need for frequent transportation of oocytes. Microfluidic fertilization has been successfully employed with pig and mouse oocytes using a narrow channel design to trap oocytes and expose these to sperm for fertilization with continuous media flow (Clark et al. 2005; Suh et al. 2006; Han et al. 2010). During the process, oocytes are exposed to flow and are held stationary by channel walls against the flow, thus viscous stresses from external flow and mechanical stresses from channel walls due to trapping are experienced by oocytes. The continuous exposure of oocytes to liquid flow may lead to significant shape deformations as well as spindle damage that may result in failure of oocyte fertilization or normal embryo development. Potential effects of shear flow and mechanical restrictions on oocytes in microfluidic channels remain to be characterized for rationalization of microfluidic tools for reproductive applications.

To study the deformation of oocytes, it is critical to precisely control the dynamic, physical, microenvironmental factors around a single oocyte and measure the resulting response of oocyte shape and spindle structure. Several microfluidic systems have been developed to trap and manipulate single oocytes employing microdrops, microwells, multilayer channels, micronozzles for in vitro fertilization (Han et al. 2010; Sadani et al. 2005; Zeggari et al. 2007; Heo et al. 2011; Jimenez et al. 2011). Confined microscale reservoirs were used to entrap oocytes and perform force measurements during microinjection (Liu et al. 2010). However, these devices do not allow the study of shape deformation and spindle structure change of oocytes under flow. In the present study, we demonstrate a simple microfluidic device for the controlled entrapment of oocytes. The microfluidic device allows the exposure of trapped oocytes to different flow rates. The shape deformation of oocytes can be imaged using a bright field microscope and characterized by a shape deformation index. The change in the spindle morphology of oocytes during microfluidic manipulations can be detected using fluorescence imaging of microtubules and chromosomes.

2 Materials and methods

2.1 Animals and retrieval of oocytes

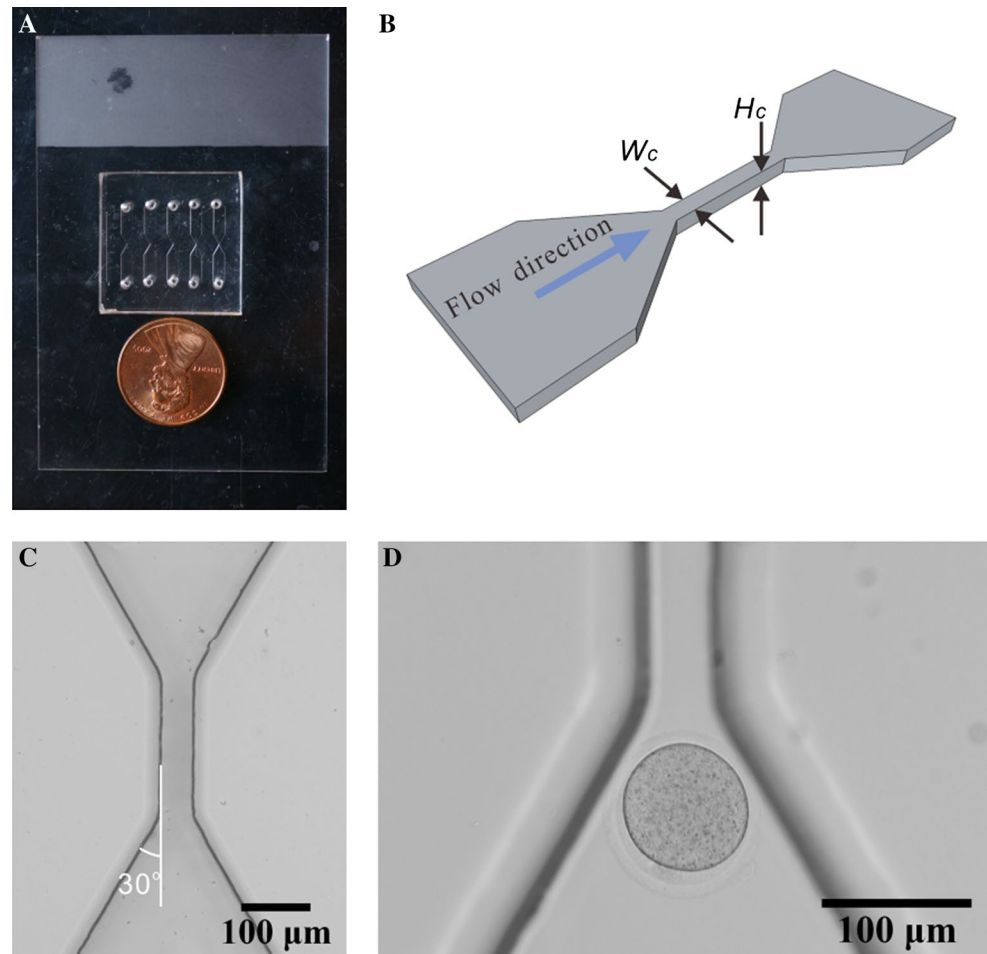
8- to 12-week-old mice of the strain B6D2F1 (Jackson Laboratory, ME, USA) were superovulated by

intraperitoneal (IP) injection of 5 IU pregnant mare serum gonadotropin (PMSG) (Sigma, MO, USA) followed 46–48 h later by IP injection of 5 IU human chorionic gonadotrophin (hCG) (Sigma, MO, USA) under the guidance of Harvard Medical School Office of Research Subject Protection (protocol number 04444). PMSG and hCG were prepared in phosphate-buffered saline (PBS) and 5 IU in 200 μ L were gently injected into the peritoneal cavity of mice. 16–18 h subsequent to hCG injection, mice were euthanised. The ovaries and oviducts were located following the tubes connecting to the Y-shaped uterus. After the adipose tissue around the ovaries was removed, the oviducts were excised and placed into a Costar[®] 60-mm center-well culture dish (Corning, MA, USA) containing pre-warmed (37 °C) EmbryoMax[®] FHM 4-(2-hydroxyethyl)piperazine-1-ethanesulfonic acid (HEPES)-buffered medium (Millipore Corporation, Billerica, MA, USA) supplemented with 4.0 mg/mL bovine serum albumin (BSA). By pricking the oviduct ampulla with a 27-gauge needle (BD, MA, USA), cumulus-oocyte complexes were released into FHM medium. The surrounding cumulus cells were removed by gently washing the cumulus-oocyte complexes to 0.3 mg/mL hyaluronidase solution (Irvine Scientific, CA, USA) in FHM medium. Cumulus-free oocytes with normal morphology were transferred into a center-well culture dish (Corning, MA, USA) containing 1 mL FHM medium. The dish containing the oocytes was placed in an incubator or on Premiere[®] slide warmer XH-2002 (Microscopes America, GA, USA) to keep the temperature at 37 °C before use. The average oocyte size was measured from 32 oocytes collected from 12 B6D2F1 mice (Figure S1).

2.2 Microfluidic device fabrication

The microfluidic device was fabricated in poly(dimethylsiloxane) (PDMS) using the photolithography techniques previously described in the literature (Tasoglu et al. 2014). Briefly, the channel structure was generated using a computer-aided design program and then was printed onto transparencies as a photomask using a commercial service (Fineline imaging, CO, USA). Using the photomask, a 150- μ m-thick layer of SU8 photoresist (MicroLithography, MA, USA) was spin-coated onto a silicon wafer (University wafer, MA, USA), which served as a master for PDMS mold fabrication. To prevent irreversible bonding to PDMS mold surface, the surface of the wafer was treated with trichloro(1H,1H,2H,2H-perfluorooctyl)silane (Sigma, MO, USA). A mixture of liquid PDMS prepolymer and curing agent (Dow Corning, MI, USA) at a weight ratio of 10:1 was then poured onto the silicon wafer.

Fig. 1 Microfluidic device and microchannels used in this study. **a** Photograph of a microfluidic device. The micro-fabricated PDMS device with five microchannels was bound to a glass slide to form closed chambers. The *bright circles (inlets and outlets)* indicate the location of the microchannels within PDMS. **b** Schematic illustrating the geometry of the microchannel with a constricted segment used to trap a single oocyte. The width and height of the constricted segment of the channel are denoted by $W = 50 \mu\text{m}$ and $H = 150 \mu\text{m}$. **c** Microscope image of the constricted segment of the channel. **d** An oocyte is trapped at the entrance of the channel constriction. Oocyte trapping is showed in Video S1



After being cured at $80\text{ }^{\circ}\text{C}$ for 1 h, the PDMS mold was peeled off and inlets and outlets were formed by a 1.5-mm puncher (Acuderm, FL, USA). After being exposed to oxygen plasma for 30 s in a plasma chamber (Harrick, NY, USA), the PDMS mold and a 50×75 mm glass slide (VWR, NY, USA) were bond together at $80\text{ }^{\circ}\text{C}$ for 30 min to achieve the final form of the microfluidic device. The microfluidic device was kept in dust free environment until use. Each device contained five microchannels (Fig. 1a).

2.3 Trap and deformation of oocytes in a flow channel

The workstation setup for the test of oocyte deformation under flow included a syringe pump (Harvard Apparatus PHD, 2000, Holliston, MA) for flow control, a stage for device position control and an inverted light microscope for oocyte visualization (Figure S2). The microchannel was first filled with phosphate-buffered saline (PBS) containing 2 % (w/v) BSA. Using a micropipette with a $125\text{-}\mu\text{m}$ stripper tip (Origio, VA, USA), a mature oocyte was transferred from the center-well dish on the hot plate at

$37\text{ }^{\circ}\text{C}$ into the inlet of a microchannel. A 1-mL syringe (BD, MA, USA) containing PBS with 2 % (w/v) BSA was inserted to the channel inlet by tubing with outer diameter of 1.524 mm. The flow rate in the microchannel was set to $5\text{--}15\ \mu\text{L}/\text{min}$ to push the oocyte toward the constricted segment. Once the oocyte approached the entrance point of the constricted segment, the flow rate was decreased to $1\text{--}2\ \mu\text{L}/\text{min}$ to trap the oocyte without deformation (Video S1). The deformation of the oocyte under various flow rates (e.g., 10 and $20\ \mu\text{L}/\text{min}$) was then observed and recorded by a microscope-coupled camera (Axio observer D1, Zeiss). The flow was terminated once the oocyte went through the constricted segment. The oocyte was then collected from the outlet using a micropipette with a stripper tip and was immediately transferred into U-bottom 96-well plate (BD, MA, USA) with fixative for further spindle immunostaining.

2.4 Spindle staining

The fixation and immunostaining of oocytes were carried out in U-bottom 96-well plates by using a micropipette

with a 125- μm stripper. Oocytes were first fixed in 4 % paraformaldehyde (Sigma, MO, USA) in PBS at room temperature for 10–30 min. Fixed oocytes were washed for 5–10 min and were then placed in a blocking solution (PBS supplemented with 2 % (w/v) BSA, 2 % (v/v) normal goat serum, 0.2 % (w/v) skim milk powder, 100 mmol/L glycine, 0.2 % (v/v) Triton X-100 and 0.2 % (w/v) sodium azide) (Navarro et al. 2005) for 1 h at room temperature. For the microtubule staining, oocytes were incubated with monoclonal anti- β -tubulin antibody (Sigma, MO, USA) diluted 1:50 in the blocking solution at 37 °C for 1 h. After being washed in the blocking solution for 5–10 min, the oocytes were incubated with Alexa 488—labeled goat anti-mouse IgG (Invitrogen, NY, USA) diluted 1:100 in the blocking solution at 37 °C for 40 min. For DNA staining, the oocytes were incubated with 4',6-diamidino-2-phenylindole (DAPI) (Sigma, MO, USA) diluted 1:100 in the blocking solution for 15–30 min. To decrease background staining, the oocytes were washed in the blocking solution twice (5–10 min for each). After washing away the remnants, oocytes were mounted in between two slides, the inter gap of which was filled with 15 μL anti-fade solution (PBS containing 50 % (v/v) glycerol and 25 mg/mL sodium azide). The oocytes were immediately imaged after mounting to avoid the fading of spindle staining color. Microtubules stained by Alexa and chromosomes stained by DAPI were presented in green and blue color, respectively. The fluorescent micrographs of oocyte spindles were obtained via an epifluorescence microscope (Carl Zeiss observer D1 model Axio inverted microscope).

3 Results and discussion

We have built a microfluidic device that can trap a single mouse oocyte for studying its morphological deformation of single oocyte under a controlled hydrodynamic flow (Fig. 1a). The microfluidic device consists of five independent channels each with a length (L) of 20 mm and a width (W) of 2 mm allowing loading and flowing of the sample (Fig. 1b). A constricted segment that has a much smaller width ($W_c = 50 \mu\text{m}$) than the main channel ($W = 2 \text{ mm}$) is fabricated in the middle of each channel to trap the oocytes (Fig. 1c, d). Oocytes can be trapped at the entrance of the constricted segment, the width (W_c) of which is smaller than oocyte diameter, by applying a relatively low flow rate, e.g., 1.0 $\mu\text{L}/\text{min}$ for a channel with a height (H_c) of 100 μm (Video S2). Subsequently, by applying a higher flow rate (e.g., 1.5 $\mu\text{L}/\text{min}$ for H_c of 100 μm), enforcement of the trapped oocyte into the segment can be achieved (Video S3). As the average diameter of B6D2F1 mouse oocyte is about 100 μm (Zhang et al. 2012) (Figure S1) and the width of the constricted segment is only 50 μm , oocytes can be significantly deformed while passing through the channel. The height of the channel (H_c) is 150 μm , unless stated otherwise, allowing exposure of the oocyte to fluids passing through the gap between the trapped oocyte and channel walls.

The degree of the deformation of a single oocyte was quantified by a deformation index (D), which is used to characterize shape changes in vesicles or blood cells under flow (Luo et al. 2013; Deschamps et al. 2009; Abkarian et al. 2007). The index helps to compare the oocyte shape evolved over time to its initial spherical shape (Fig. 2a). D values during the deformation of an oocyte can be calculated as:

Fig. 2 Characterization of oocyte deformation in the microfluidic channel. **a** Time sequence of video images of an oocyte deformed in the channel with a constricted segment of $W = 50 \mu\text{m}$ and $H = 100 \mu\text{m}$. **b** Schematic of the length L_o and the width B_o of the deformed oocyte. **c** Time evolution of L_o and B_o , and a dimensionless parameter (deformation index D) defined as $D = (L_o - B_o)/(L_o + B_o)$. The increase in D with time demonstrates the increase in the degree of deformation of the oocyte presented in (a). The scale bar in (a) is 100 μm

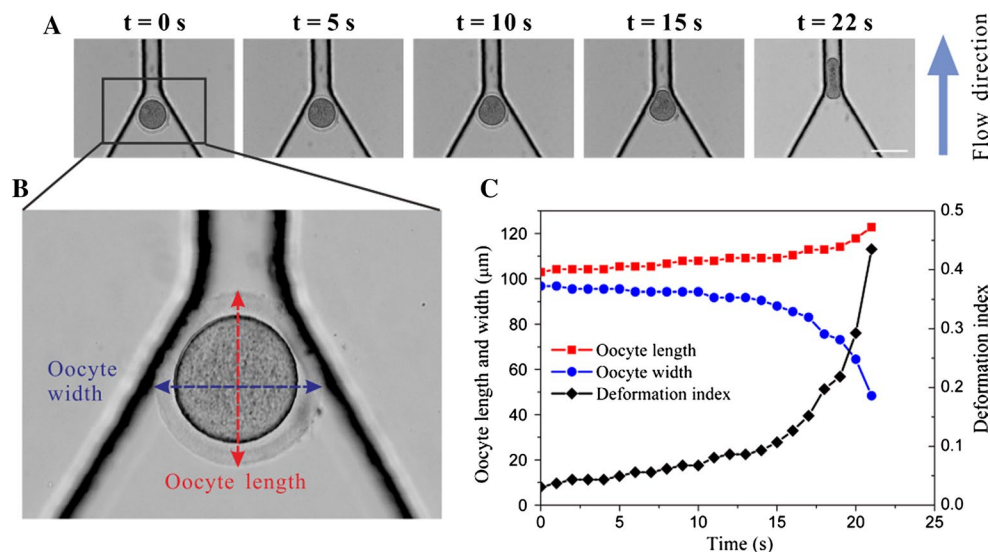
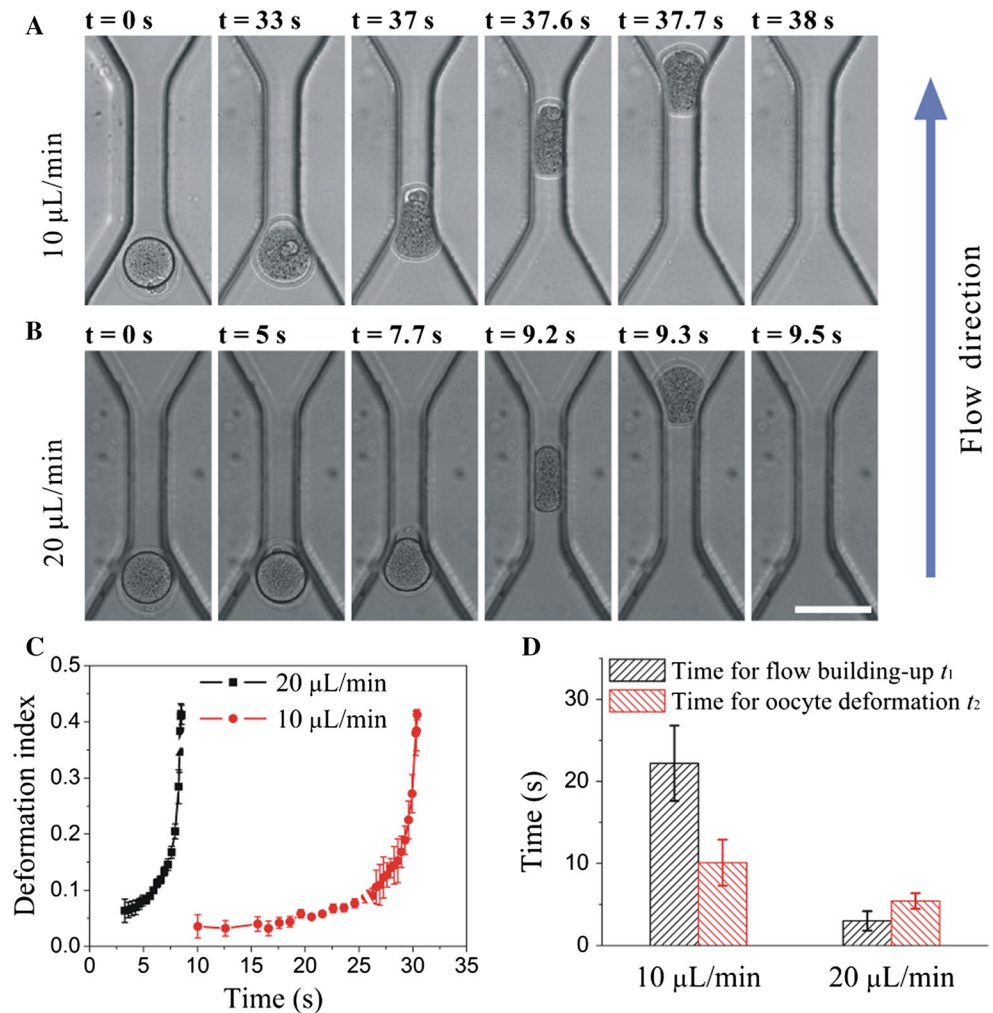


Fig. 3 Transient deformation of trapped oocytes under different flow rates. **a, b** are time sequence images of oocytes deformed in a constricted channel with $W = 50 \mu\text{m}$ and $H = 150 \mu\text{m}$. The flow rate is **a** $10 \mu\text{L}/\text{min}$ and **b** $20 \mu\text{L}/\text{min}$. The scale bar is $100 \mu\text{m}$. **c** Time evolution of the deformation index D . **d** The time period Δt_1 between the starting of the flow pump and the beginning of oocyte deformation and the time period Δt_2 between the beginning of oocyte deformation and the going through of the oocyte



$$D = \frac{L_o - B_o}{L_o + B_o}$$

where L_o is the length and B_o is the width of the deformed oocyte (Fig. 2b). When the oocyte is not deformed, it is nearly spherical and the value of D therefore is close to zero. The time evolution of D during the deformation of a single oocyte is shown in Fig. 2c. During the penetration of the oocyte into the constricted segment, L_o increases and B_o decreases, resulting in an increasing deformation index (Fig. 2c). As shown in Fig. 2a, b, the oocyte shows a nearly spherical shape at the entrance of the constricted segment ($t = 0 \text{ s}$), with a deformation index of $D = 0.03$. Until $t = 15 \text{ s}$, the oocyte is gradually elongated in the direction of the flow and is deformed to a non-spherical shape, with D increasing to 0.11 (Fig. 2c). From $t = 15 \text{ s}$ to $t = 21 \text{ s}$, the oocyte is rapidly elongated until it is entirely in the constricted segment and gets significantly deformed, with D rapidly increasing to 0.43 (Fig. 2c).

To correlate the magnitude of hydrodynamic pressure to the deformation of an oocyte, we expose trapped oocytes to

two different flow rates: 10 and 20 $\mu\text{L}/\text{min}$. The deformation index of oocytes under different flow rates are demonstrated in Fig. 3. Under both flow conditions, the oocytes are deformed (Fig. 3a, b) and the increase in D shows similar increasing tendency (Fig. 3c) as in Fig. 2c. The time required by the oocyte to pass through the constricted segment (Δt) from the time of entry until the exit of the oocyte from the segment significantly decreases with increasing flow rate (Fig. 3c). There is a lag time starting from the time when the flow pump is activated until the entry of the oocyte into the constricted segment. During this time, the oocyte shows no significant deformation (Videos S4 and S5). Thus, we have sub-categorized the time Δt into two durations: (1) Δt_1 representing the time period until the entry of oocyte into the constricted segment and (2) Δt_2 representing the time period from the beginning of oocyte deformation until the exit of the oocyte from the constricted segment. As the flow rate increases by twofold from 10 to 20 $\mu\text{L}/\text{min}$, Δt_1 decreases from 22.2 to 3.0 s and Δt_2 decreases from 10.1 to 5.4 s (Fig. 3d). The speed of deformation of the trapped oocyte significantly increases with

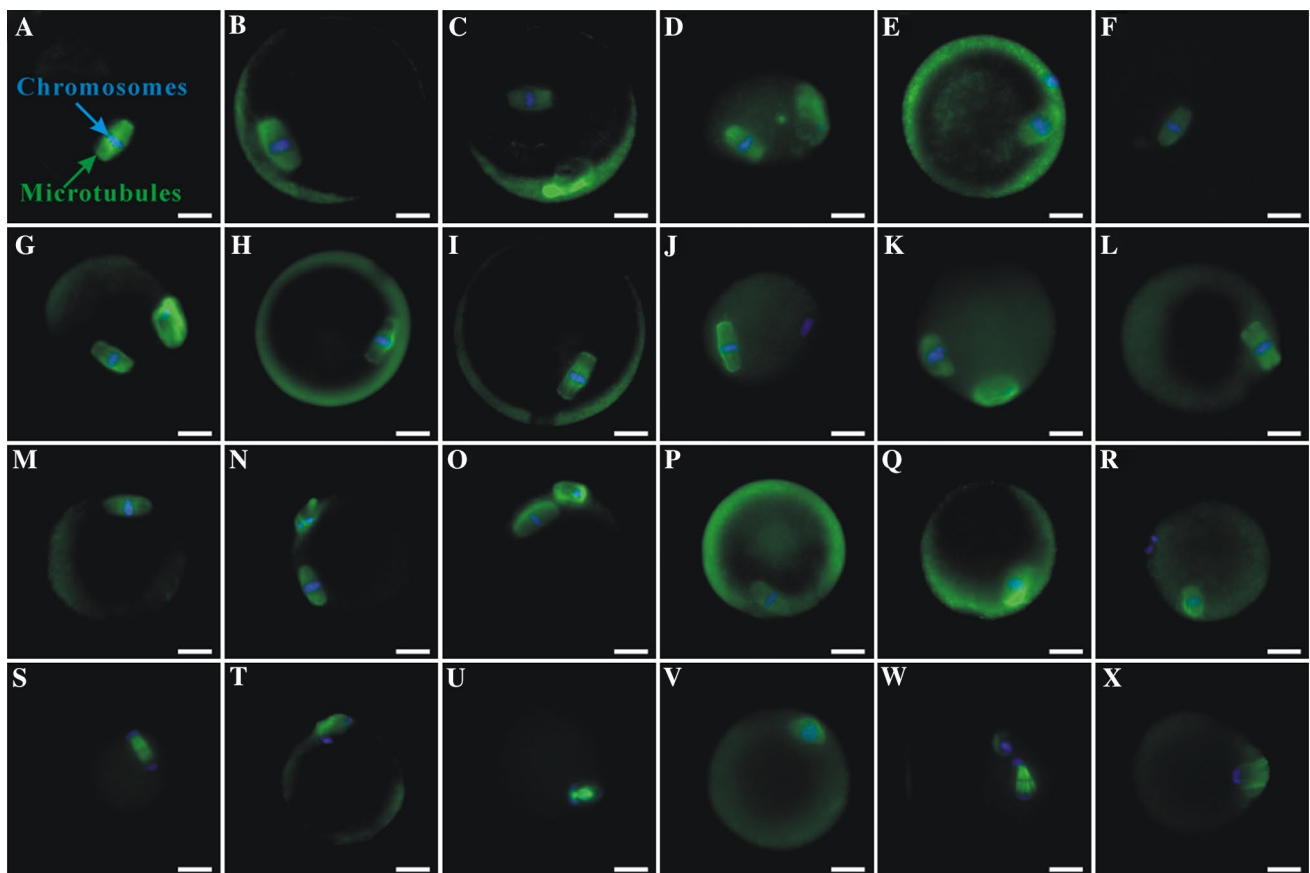


Fig. 4 Fluorescence microscopy images showing changes in spindle structure (green) and chromosomal alignment (blue) in oocytes. (a–f) Normal spindle structure in fresh oocytes as a control. (g–l) Normal spindle structure in fresh oocytes incubated at room temperature for 30 min as another control to eliminate the effect of temperature on

the spindle. (m–x) Oocytes collected from the microfluidic device that went through the channel constriction. (m–r) are oocytes with normal spindles, and (s–x) are oocytes with abnormal or damaged spindle structures. The scale bar is 20 μm

increasing flow rate in the microchannel. This higher flow rate leads to a higher hydrodynamic pressure on the oocyte (Thomas and Bolton 1999; Kim et al. 2006). It is noteworthy that, compared with the condition of $H_c = 150 \mu\text{m}$, the oocyte can go through the channel constriction with $H_c = 100 \mu\text{m}$ at much lower flow rate (i.e., 1.5 $\mu\text{L}/\text{min}$). Besides, the time period of the oocyte deforming process $\Delta t_2 = 15.9 \text{ s}$ at $H_c = 100 \mu\text{m}$ and flow rate of 1.5 $\mu\text{L}/\text{min}$ is much longer than that at larger channel height of $H_c = 150 \mu\text{m}$ for both flow rates of 10 and 20 $\mu\text{L}/\text{min}$. Nevertheless, at the two different channel heights of 100 and 150 μm , the deformation degree of oocytes showed similar increasing tendency with time and the maximum value of oocyte deformation were close, i.e., $D = 0.43$ at $H_c = 100 \mu\text{m}$ and $D = 0.42$ at $H_c = 150 \mu\text{m}$. Previous studies on mechanical behavior of oocytes focus on oocytes under no-flow conditions using microinjector (Liu et al. 2010; Sun et al. 2003; Papi et al. 2010), while it is hard to use microinjector for studying mechanical behavior of oocytes under flow conditions. Here, we demonstrated a

simple platform that can be used to study the flow effects on a single oocyte during external shear flow, which can be helpful for manipulating oocytes in microfluidic flow.

We further analyzed the change in the spindle morphology of oocytes to evaluate the potential spindle damage due to the hydrodynamic flow. We recovered the oocytes from the outlet of microfluidic channels and stained the microtubules and chromosomes (Fig. 4). Spindles of oocytes which have passed through the channels have been compared to spindles of freshly retrieved healthy oocytes (Fig. 4a–f). In fresh oocytes, microtubules (green) are organized into a barrel shape and chromosomes (blue) are arranged into a compact plane in the middle of the microtubule assembly (Fig. 4a). Temperature is an essential factor that affects the integrity of the spindle during in vitro manipulation of oocytes (Wang et al. 2001; Zenzes et al. 2001; Raju et al. 2007). The optimum temperature for handling and culturing of oocytes is 37 $^{\circ}\text{C}$. We performed our microscopy experiments at room temperature ($\sim 25 \text{ }^{\circ}\text{C}$) for time periods less than 30 min. We considered the potential effect of this

temperature drop in spindle structure and created a secondary control group using freshly retrieved healthy oocytes incubated at room temperature for 30 min. Spindles of these oocytes exhibit normal structure (Fig. 4g–l), which is similar to that in fresh oocytes (Fig. 4a–f). Therefore a possible destruction of spindle by a change in the ambient temperature was not observed. The oocytes that have passed through the constricted segment in the channel exhibit both undamaged (Fig. 4m–r) and damaged (Fig. 4s–x) spindle structures. The chromosomes of damaged spindles are broken into several parts and dislocated from the middle plane of the spindle (Fig. 4s–u, w) or are not collectively arranged into a compact plane at the center of the spindle (Fig. 4v). The shape of the spindle can be deformed from a symmetric barrel shape to various asymmetric shapes (Figs. 4t–u, w–x). The percentage of oocytes with normal spindle structure (Fig. 4a–l) is 80 and 83.9 % for two control groups, i.e., fresh oocytes ($N = 35$) and oocytes incubated at room temperature for 30 min ($N = 31$), respectively (Figure S3). The percentage of oocytes ($N = 34$) with normal spindle structure collected from the microfluidic device is 41.2 % (Fig. 3m–r). Five in 10 oocytes exposed to flow condition of 10 $\mu\text{L}/\text{min}$ still have normal spindle structure, and the ratio is 3/7 for 20 $\mu\text{L}/\text{min}$. In the present study, the spindle damage is mainly due to the flow-induced significant deformation of the oocyte going through the channel constriction. The maximum deformation of oocytes at the two flow rates of 10 and 20 $\mu\text{L}/\text{min}$ is similar (Fig. 3), and thus the percentage of oocytes with normal spindle at both flow rates is much lower than the two control groups. In the future work, the impact of shear stresses on spindle organization of oocytes without significant deformation can be studied by using the present microfluidic channel design with larger channel height. In this study, we observed abnormal spindle morphologies induced by the deformation of the oocyte. Although some literature studied the mechanical damage on oocytes by focusing particularly on microinjection to guide intracytoplasmic sperm injection technique (Dumoulin et al. 2001; Ebner et al. 2003), we presented the damage on oocytes under flow with wall interactions through a constricted segment, which can be potentially useful for the development of microfluidics-based in vitro fertilization techniques and for establishing design parameters for oocyte manipulation.

It is demonstrated in this study that single oocytes exhibit significant deformation in the constricted microfluidic channel under the push of the flow. The oocyte cytoskeleton composed of a network of fibers in the cytoplasm connects the oocyte membrane and the spindle together, and hence large deformation of the oocyte can easily induce abnormal structures of the spindle. During ICSI, techniques (e.g., use of cytochalasin B) have often been used to relax the cytoskeleton and enhance the flexibility of oocytes (Sun

and Schatten 2006; Hu et al. 2012), which can increase the successful rate of in vitro fertilization. Thus, it is interesting to study the impact of shear flows on the spindle organization of cytochalasin B-treated oocytes in the future work. Besides, it should be noted that during ICSI, conventional IVF and microfluidics-based IVF, the oocytes may not undergo shape deformation at the level demonstrated in this study, though they are usually exposed to shear flows. Thus, there is still an unmet need in studying the influence of constant flow on the spindle organization while maintaining the oocytes nearly spherical to fully understand the impact of oocyte manipulation, e.g., washing or transferring of oocytes into fresh medium during IVF and stabilization of an oocyte using micropipette during ICSI. The simple design of the microfluidic channel can be useful in these future studies due to its ability of trapping single oocyte and applying shear flow on the oocyte.

This work reports the deformation of a single oocyte under microfluidic flow condition by developing a simple microfluidic device with a constricted segment narrowed in the channel width direction. It is noteworthy that a channel integrating a constricted segment narrowed in the channel height direction was used to trap the oocyte for fertilization (Clark et al. 2005). However, it is hard to observe the deformation of a trapped oocyte in the aforementioned channel structure using a conventional microscope, as the major distortion occurs in the channel height direction. The simple microfluidic device presented in this study can be further developed for mechanical characterization of single oocytes by measuring the hydrodynamic pressure differences, which is similar in operating principles to a microfluidic system for evaluating red blood cell deformability (Assal et al. 2014). Besides, this microfluidic device can be used to study spindle damage in other cell types by changing the size of the constricted segment to be smaller than the size of target cells.

4 Conclusion

We developed a single oocyte trapping microfluidic device that is capable of studying the deformation of single oocytes induced by hydrodynamic pressure and mechanical restriction. A microchannel with a constricted segment enables to observe the deformation of a single oocyte trapped at the entrance of the constricted segment. The device can be coupled to a conventional light microscope to observe the deformation of oocytes. The microfluidic device allows the retrieval of oocytes after flow, and hence, the structure and function of internal components, for example spindle, can be labeled and evaluated. The microfluidic device can be used in future studies to investigate the impact of several other characteristic parameters during single oocyte manipulation such as tension of cortex and hardening of zona pellucida.

Acknowledgments Utkan Demirci acknowledges that this work is supported by the National Institutes of Health award (R01 EB015776). We would like to acknowledge Dr. Aida Nureddin for her significant contributions to this work. ZhengYuan Luo acknowledges financial supports from China Scholarship Council. This work was also partially supported by Swedish Research Council Vetenskapsrådet.

Conflict of interest Dr. Utkan Demirci is a founder of and has an equity interest in: (1) DxNow Inc., a company that is developing microfluidic and imaging technologies for point-of-care diagnostic solutions, and (2) Koek Biotech, a company that is developing microfluidic IVF technologies for clinical solutions. Dr. Utkan Demirci's interests were viewed and managed by the conflict of interest policies.

References

- Abkarian M, Favre M, Viallat A (2007) Swinging of red blood cells under shear flow. *Phys Rev Lett* 98:188302
- Asghar W, Velasco V, Kingsley JL, Shoukat MS, Shafiee H, Anchan RM, Demirci U (2014) Selection of functional human sperm with higher DNA integrity and fewer reactive oxygen species. *Adv Healthc Mater*. doi:10.1002/adhm.201400058
- Assal RE, Guven S, Gurkan UA, Gozen I, Shafiee H, Dalbeyler S, Abdalla N, Thomas G, Fuld W, Illigens BMW, Estanislau J, Khoory J, Kaufman R, Zylberberg C, Lindeman N, Wen Q, Ghiran I, Demirci U (2014) Bio-Inspired Cryo-Ink Preserves Red Blood Cell Phenotype and Function During Nanoliter Vitrification. *Adv Mater*. doi:10.1002/adma.201400941
- Clark SG, Haubert K, Beebe DJ, Ferguson CE, Wheeler MB (2005) Reduction of polyspermic penetration using biomimetic microfluidic technology during in vitro fertilization. *Lab Chip* 5:1229–1232
- Deschamps J, Kantsler V, Segre E, Steinberg V (2009) Dynamics of a vesicle in general flow. *Proc Natl Acad Sci USA* 106:11444–11447
- Dumoulin JCM, Coonen E, Bras M, Bergers-Janssen JM, Ignoul-Vanvuchelen RCM, van Wissen LCP, Geraedts JPM, Evers JLH (2001) Embryo development and chromosomal anomalies after ICSI: effect of the injection procedure. *Hum Reprod* 16:306–312
- Ebner T, Moser M, Sommergruber M, Puchner M, Wiesinger R, Tews G (2003) Developmental competence of oocytes showing increased cytoplasmic viscosity. *Hum Reprod* 18:1294–1298
- El-Ali J, Sorger PK, Jensen KF (2006) Cells on chips. *Nature* 442:403–411
- Gurkan UA, Tasoglu S, Akkaynak D, Avci O, Unluisler S, Canikyan S, MacCallum N, Demirci U (2012) Smart interface materials integrated with microfluidics for on-demand local capture and release of cells. *Adv Healthc Mater* 1:661–668
- Han C, Zhang Q, Ma R, Xie L, Qiu T, Wang L, Mitchelson K, Wang J, Huang G, Qiao J, Cheng J (2010) Integration of single oocyte trapping, in vitro fertilization and embryo culture in a microwell-structured microfluidic device. *Lab Chip* 10:2848–2854
- Heo YS, Lee H-J, Hassell BA, Irimia D, Toth TL, Elmoazzen H, Toner M (2011) Controlled loading of cryoprotectants (CPAs) to oocyte with linear and complex CPA profiles on a microfluidic platform. *Lab Chip* 11:3530–3537
- Hu L-L, Shen X-H, Zheng Z, Wang Z-D, Liu Z-H, Jin L-H, Lei L (2012) Cytochalasin B treatment of mouse oocytes during intracytoplasmic sperm injection (ICSI) increases embryo survival without impairment of development. *Zygote* 20:361–369
- Jimenez AM, Roche M, Pinot M, Panizza P, Courbin L, Gueroui Z (2011) Towards high throughput production of artificial egg oocytes using microfluidics. *Lab Chip* 11:429–434
- Kim T, Wang CW, Thomas FIM, Sastry AM (2006) Fluid-structure interaction analysis of flow-induced deformation in a two-phase, Neo-Hookean marine egg. *J Eng Mater-T ASME* 128:519–526
- Lathi RB, Milki AA (2004) Rate of aneuploidy in miscarriages following in vitro fertilization and intracytoplasmic sperm injection. *Fertil Steril* 81:1270–1272
- Liu X, Fernandes R, Jurisicova A, Casper RF, Sun Y (2010) In situ mechanical characterization of mouse oocytes using a cell holding device. *Lab Chip* 10:2154–2161
- Luo ZY, Wang SQ, He L, Lu TJ, Xu F, Bai BF (2013) Front tracking simulation of cell detachment dynamic mechanism in microfluidics. *Chem Eng Sci* 97:394–405
- Navarro P, Liu L, Trimarchi JR, Ferriani RA, Keefe DL (2005) Non-invasive imaging of spindle dynamics during mammalian oocyte activation. *Fertil Steril* 83:1197–1205
- Papi M, Brunelli R, Sylla L, Parasassi T, Monaci M, Maulucci G, Missori M, Arcovito G, Ursini F, De Spirito M (2010) Mechanical properties of zona pellucida hardening. *Eur Biophys J Biophys* 39:987–992
- Raju GAR, Prakash GJ, Krishna KM, Madan K (2007) Meiotic spindle and zona pellucida characteristics as predictors of embryonic development: a preliminary study using PolScope imaging. *Reprod Biomed Online* 14:166–174
- Rizvi I, Gurkan UA, Tasoglu S, Alagic N, Celli JP, Mensah LB, Mai Z, Demirci U, Hasan T (2013) Flow induces epithelial-mesenchymal transition, cellular heterogeneity and biomarker modulation in 3D ovarian cancer nodules. *Proc Natl Acad Sci USA* 110:E1974–E1983
- Sadani Z, Wacogne B, Pieralli C, Roux C, Gharbi T (2005) Microsystems and microfluidic device for single oocyte transportation and trapping: toward the automation of in vitro fertilising. *Sensor Actuat A-Phys* 121:364–372
- Suh RS, Zhu XY, Phadke N, Ohl DA, Takayama S, Smith GD (2006) IVF within microfluidic channels requires lower total numbers and lower concentrations of sperm. *Hum Reprod* 21:477–483
- Sun QY, Schatten H (2006) Regulation of dynamic events by microfilaments during oocyte maturation and fertilization. *Reproduction* 131:193–205
- Sun Y, Wan KT, Roberts KP, Bischof JC, Nelson BJ (2003) Mechanical property characterization of mouse zona pellucida. *IEEE Trans Nanobiosci* 2:279–286
- Tasoglu S, Gurkan UA, Wang S, Demirci U (2013a) Manipulating biological agents and cells in micro-scale volumes for applications in medicine. *Chem Soc Rev* 42:5788–5808
- Tasoglu S, Safaee H, Zhang X, Kingsley JL, Catalano PN, Gurkan UA, Nureddin A, Kayaalp E, Anchan RM, Maas RL, Tuetzel E, Demirci U (2013b) Exhaustion of racing sperm in nature-mimicking microfluidic channels during sorting. *Small* 9:3374–3384
- Tasoglu S, Diller E, Guven S, Sitti M, Demirci U (2014) Untethered micro-robotic coding of three-dimensional material composition. *Nat Commun* 5:3124
- Thomas FIM, Bolton TF (1999) Shear stress experienced by echinoderm eggs in the oviduct during spawning: potential role in the evolution of egg properties. *J Exp Biol* 202:3111–3119
- Vanapalli SA, Duits MHG, Mugele F (2009) Microfluidics as a functional tool for cell mechanics. *Biomicrofluidics* 3:012006
- Wang WH, Meng L, Hackett RJ, Odenbourg R, Keefe DL (2001) Limited recovery of meiotic spindles in living human oocytes after cooling-rewarming observed using polarized light microscopy. *Hum Reprod* 16:2374–2378
- Zeggari R, Wacogne B, Pieralli C, Roux C, Gharbi T (2007) Microfluidic applications for andrology. *Sensor Actuat B-Chem* 125:664–671
- Zenzes MT, Bielecki R, Casper RF, Leibo SP (2001) Effects of chilling to 0 degrees C on the morphology of meiotic spindles in human metaphase II oocytes. *Fertil Steril* 75:769–777
- Zhang X, Khimji I, Shao L, Safaee H, Desai K, Keles HO, Gurkan UA, Kayaalp E, Nurreddin A, Anchan RM, Maas RL, Demirci U (2012) Nanoliter droplet vitrification for oocyte cryopreservation. *Nanomedicine* 7:553–564